Fracture 1977, Volume 1, ICF4, Waterloo, Canada, June 19 - 24, 1977

MICRO AND MACRO FRACTURE MECHANICS APPROACH TO BRITTLE FRACTURE AND FATIGUE CRACK GROWTH

T. Yokobori, S. Konosu and A. T. Yokobori, Jr.*

ABSTRACT

From the reasoning of the essential varieties of the fracture types, it should be considered accordingly that there will be an inevitable variety of fracture criteria. Also, the model for the mechanism of crack growth will be different by different input such as stress or strain level, temperature range, loading velocity, etc. The classification being made, in the present article, a combined micro- and macro fracture mechanics approach has been made to the criterion for brittle fracture and for fatigue crack growth as typical examples of so-called time independent and time dependent fracture respectively.

INTRODUCTION

From the reasoning of the essential varieties of the fracture types, it should be considered accordingly that there will be an inevitable variety of fracture criteria. A classification has been attempted as recorded in Table 1. Models for the mechanism of crack growth will also be different through different inputs such as level of stress, strain, temperature range, loading velocity, etc.: these are classified in Figure 1, [1].

Turning to micro and macro aspects, real materials contain defects of two kinds as stress raisers, that is, cracks as macroscopic defect and crystal lattice dislocations as microscopic defects. Usually fracture mechanics, however, is concerned explicitly with one of these two factors. For instance, continuum mechanics, such as L F M concerns the crack, the microscopic factor being wholely confined to the "black box". On the contrary, dislocation mechanics concerns only the microscopic factor, and not the macroscopic crack.

In the present article, a combined micro - and - macro fracture mechanics approach has been made to the criterion for brittle fracture (the case of Table 1, type 1) and for fatigue crack growth (the case of Table 1, type 4) as typical examples of so called time independent and time dependent fracture, respectively.

MICRO AND MACRO FRACTURE MECHANICS APPROACH TO BRITTLE FRACTURE

For the case of fracture under unidirectional and single loading, in which applied stress plays a governing role and which is not so much affected by thermal activation, the following two requisites should be satisfied.

*Department of Mechanical Engineering II, Tohoku University, Sendai, Japan.

The first requisite is the *energy* requisite, which means the energy balance condition. The second requisite is the *critical local stress* requisite, which means that the local stress at or near the tip of the crack should exceed the ideal strength, that is, atomic cohesion. However, linear elasticity fracture mechanics and J_c fracture mechanics assume only the energy requisite. On the contrary, the criterion for the fracture of this type will be given by the most critical one of the two mentioned above. In this section let us consider the case in which the rate controlling process for the crack growth or fracture is given by the separation mechanism of opposed atoms normal to the atomic planes by tensile stress, say, the case of brittle fracture (Table 1, type 1).

Let us consider a configuration of a main crack and a slip band as shown in Figure 2 as a critical model for crack growth which corresponds to the model (b) or (d) in Figure 1. Energy requisite and critical local stress requisite were obtained for crack propagation occurring from each tip opposed between the main crack and the slip band respectively. Thus four applied critical stresses were derived [2] corresponding to each four requisities obtained above. The requisite leading to the highest value of the four critical stresses will never be satisfied before growth of the main crack will occur. That is, the crack initiation and/or extension will not occur from the tip concerned before the crack initiation and/or extension will occur from the other opposite tip between main crack and the slip band. In this way we can determine whether growth of the main crack will start from the slip band tip (Figure 1b or 1b') or from the main crack tip itself (Figure 1d).

As a result of this line of analysis, the following two features are deduced: For the case of the main crack with the larger radius of the tip, the crack growth mechanism is that the microcrack will initiate near the opposed slip band tip and propagate, joining the main crack as shown in Figure 1b, [2]. On the other hand, for the case of the main crack with the smaller radius of the tip, the crack growth mechanism is that the opposed tip of the main crack itself will extend as shown in Figure 1d, [3]. It is interesting to note that for the case of both types the criterion for crack propagation or growth, that is, fracture criterion is given in fairly good approximation as the following formula [2], [3]:

$$K_c = \sqrt{2E\gamma_p^*} \tag{1}$$

which is apparently similar to that by linear fracture mechanics. However, the formula is remarkably different from conventional fracture mechanics in that γ_p^* is analytically expressed in terms of atomic, microstructural and macroscopic or continuum parameters as shown in Table 2. The comparison of the analysis with the experimental data shows that the criterion is in good agreement with the experimental characteristics on the effects of ferrite grain size [3], (Figure 3), the crack tip radius and the crack length on the fracture stress or fracture toughness in brittle fracture of steels.

It is to be noted that this mechanics may be applied not only to linear elasticity, but also to nonlinear fracture mechanics.

MICRO AND MACRO FRACTURE DYNAMICS APPROACH TO FATIGUE CRACK GROWTH

For the case of crack growth under alternating loading in which thermal activation plays a role, the requisite for crack growth will be given in terms of the one and the same equation [1] involving both energy balance

and local critical stress breaking concepts. Thus the requisite itself becomes the criterion (Table 1, types 2 and 4). In this section let us consider the case in which the rate controlling process for fatigue crack growth rate is given by the slip mechanism between the opposed atoms parallel to the atomic planes by shear stress (Table 1, type 4).

Theory

The essential base of the treatment herein is the analysis of the problem of the instability of dislocation emission from the crack tip and of the dislocation groups dynamics [4], [5], taking into account of macro fracture mechanics concept. The results of the analysis were applied to the fatigue crack model by blunting and resharpening [6] and also to the fatigue crack model in which da/dN is determined by off-set itself, for instance, the coarse slip model as proposed by Neuman [7].

With respect to the problem of the instability of dislocation emission from the crack tip, Rice and Thompson [8] assumed that at the fracture load, energy balance criterion by Griffith will just hold in the analysis of the ductile versus brittle response under so-called static fracture caused by unidirectionally increasing load. Thus they concluded that sharp cleavage crack is stable in body centered cubic metals, while blunting occurs spontaneously in face centered cubic metals. In the case of fatigue crack growth, however, there is no reason why we should assume Griffith type energy criterion fulfilment at least during each tensile stroke. Therefore, we analyzed the problem by using ordinary stress distribution formula itself without substituting such criterion. Therefore, from the standpoint of such consideration, the force $\tau_{\rho\phi}b_e$ on the dislocation segment under Mode I (tensile opening mode) should be written as:

$$f_\tau = \tau_{\rho\phi}b_e = \frac{K_I b}{\sqrt{8\pi\rho}} \sin\phi \cos(\phi/2)\cos\psi \tag{2}$$

instead of the equation (3) in Reference [6], where $\tau_{\rho\phi}$ = the shear stress acting at the distance ρ from the crack front on the slip plane. K_I = the stress intensity factor, ϕ = the angle between the slip plane and the crack plane, $b_e = b\cos\psi$ = the edge component of Burgers vector, (Figure 4). In the following, let us assume for convenience $\psi = 0°$ and $\phi = 90°$. Thus the critical distance ξ_c at which straight dislocation is in unstable equilibrium under the three forces of the applied load, the image force and the ledge force is given by the solution of

$$f_{tot} = \mu b\left(\frac{K_I}{4\mu}\frac{1}{\sqrt{\pi b\xi}} - \frac{1}{4\pi\xi}\frac{1}{1-\nu} - \frac{2\gamma}{\pi\mu b}\frac{\alpha}{\xi^2+\alpha^2}\right) = 0 \tag{3}$$

where $\xi = \rho/b$, γ = the true surface energy of the crack plane. $\alpha = e^{3/2}\xi_o/2$, and ξ_o = core cut off of dislocation. Since the value of lege force can be neglected as compared with the other two forces in equation (3), then we get

$$\xi_c = \frac{b}{\pi(1-\nu)^2}\frac{\mu^2}{K_I^2} \tag{4}$$

where μ = the shear modulus, ν = Poisson's ratio. Using the materials constants, we get $\xi_c = \frac{7.63}{K_I^2}$ and $\xi_c = \frac{1.34}{K_I^2}$ for iron and aluminum respectively.

In the case of usual fatigue testing, $K_I > 3.38$ kg mm$^{-3/2}$ for iron and $K_I > 0.82$ kg mm$^{-3/2}$ for aluminum. Thus, we get $\xi_c < \xi_o$; because $\xi_o \equiv 2/3$ for iron and $\xi_o \equiv 2$ for aluminum. Therefore, spontaneous generation of dislocation will occur, since the value of ξ_c is less than the cut off ξ_o.

Furthermore, under the condition of equation (2), the total energy change U_{act} for a crack which has emitted a dislocation loop will have a maximum when

$$\frac{dU_{act}}{dr} = \mu b^3\left(\frac{2-\nu}{8(1-\nu)}\ln\frac{er}{\xi_o} + \frac{2\gamma}{\mu b} - \frac{1}{\sqrt{2}}\frac{K_1}{\mu\sqrt{b}}\sqrt{r}\right) = 0 \ . \qquad (5)$$

The value of $\frac{dU_{act}}{dr}$ can be seen to have a maximum value in the range of $0 \leq r < +\infty$. Therefore, in order that equation (5) should hold, the following relation should be satisfied:

$$\left(\frac{dU_{act}}{dr}\right)_{max} = \mu b^3\left[\frac{2-\nu}{8(1-\nu)}\ln\left\{\frac{e}{\xi_o}\frac{1}{8}\left(\frac{2-\nu}{1-\nu}\right)^2\left(\frac{\mu\sqrt{b}}{K_1}\right)^2\right\} - \frac{2-\nu}{4(1-\nu)} + \frac{2\gamma}{\mu b}\right] \geq 0. \qquad (6)$$

On the other hand, the condition (6) requires $K_1 \leq 3.119$ kg mm$^{-3/2}$ for iron and $K_1 \leq 0.7257$ kg mm$^{-3/2}$ for aluminum. In the case of usual fatigue testing, however, $K_1 \geq 3.119$ kg mm$^{-3/2}$ for iron and $K_1 \geq 0.7257$ kg mm$^{-3/2}$ for aluminum. Therefore,

$$\frac{dU_{act}}{dr}$$

is negative for range of r concerned, that is, U_{act} will decrease with increase of r, not having the maximum value. Therefore, the emission of dislocation loop will be spontaneous with no activation energy.

Thus from the analysis mentioned above, it can be seen that in both body centered and face centered cubic metals, dislocation emission is spontaneous during tensile cycle in the case of a crack under alternating stress, that is, fatigue crack blunting occurs (Figure 5) in most of metals under Mode I as shown in many experimental data.

It can be seen from the above analysis that the crack opening displacement COD, u induced by this mechanism under Mode I is equal to 2 nb (Figure 6c), where b = Burgers vector and n = the number of dislocations emitted from the crack tip until the time concerned. On the other hand, fatigue crack growth rate da/dN in blunting and resharpening model is approximately equal to $\frac{1}{2}u$ (Figure 6), and, therefore, we get

$$\frac{da}{dN} \simeq nb \ . \qquad (7)$$

Furthermore, according to the above analysis, the relative displacement, s by slip, that is, off-set itself is equal to nb whether the condition is under Mode I or Mode II. Therefore, in Model in which da/dN mainly consists of off-set, da/dN is approximately equal to s. Thus, it is to be noted that equation (7) will hold in both blunting and resharpening model (Figure 6) and coarse slip model (Figure 7) either under Mode I or Mode II loading, for both bcc and fcc metals.

On the other hand n can be expressed by the following simple, analytical formula given by computer simulation of dislocation groups dynamics [4], [5].

$$n = \gamma(m)\left(\frac{4fb}{v_o}\right)^{-\frac{m+1}{m+2}}\left(\frac{\tau_o^*}{\mu}\right)^{-\frac{m(m+1)}{m+2}}\left(\frac{\tau_a}{\mu}\right)^{\frac{(m+1)^2}{m+2}} \qquad (8)$$

for large number* of n, where,

f = loading frequency,

τ_a = applied shear stress,

τ_o^* = a constant which represents the stress required to give v = 1 cm/sec (the resistant stress against the motion of a dislocation under cyclic stress).

m = the exponent in the dislocation velocity equation of

$$v = v_o\left(\frac{\tau_a}{\tau_o^*}\right)^m, \text{ in which } v_o = 1 \text{ cm/sec, and}$$

$\gamma(m)$ = nondimensional value depending on m, [5].

For the situation in which the dislocation is emitted from the crack surface as this case, the stress field at the crack tip should be used as the applied stress τ_a. For convenience,

$$\frac{\Delta K_1}{\sqrt{\varepsilon}}$$

may be used instead of τ_a, where the applied stress is averaged over some distance ε, and ΔK_1 is stress intensity factor in terms of stress amplitude. Using the applied stress $\tau_{ae} = \Delta K_1/\sqrt{\varepsilon}$ and equation (7), (8) thus becomes,

$$\frac{da}{dN} = b\gamma(m)\left(\frac{4fb}{v_o}\right)^{-\frac{m+1}{m+2}}\left(\frac{\tau_o^*}{\mu}\right)^{-\frac{m(m+1)}{m+2}}\left(\frac{\Delta K_1}{\sqrt{\varepsilon}\mu}\right)^{\frac{(m+1)}{m+2}} \qquad (9)$$

In the case in which the velocity of an isolated dislocation is given by thermally activated process, n is expressed in terms of an apparent single rate process [5] as follows:

$$n = A^*(4f)^{-\frac{m+1}{m+2}}\left(\frac{\Delta K_1}{\sqrt{\varepsilon}\mu}\right)^{\frac{m+1}{m+2}}\exp\left[-\frac{\left(\frac{m+1}{m+2}\right)H_k\ell n\left(\frac{\tau_{oo}\sqrt{\varepsilon}}{\Delta K_1}\right)}{4kT}\right], \qquad (10)$$

where T = absolute temperature, H_k = the kink energy, and

$$A^* = \gamma(m)\left(\frac{b}{A_1}\right)^{-\frac{m+1}{m+2}},$$

[5]. $m = H_k/(4kT)$, [9]. Thus using equation (10), the crack growth rate becomes

$$\frac{da}{dN} = bA^*(4f)^{-\frac{m+1}{m+2}}\left(\frac{\Delta K_1}{\sqrt{\varepsilon}\mu}\right)^{\frac{m+1}{m+2}}\exp\left[-\frac{\left(\frac{m+1}{m+2}\right)H_k\ell n\left(\frac{\tau_{oo}\sqrt{\varepsilon}}{\Delta K_1}\right)}{4kT}\right]. \qquad (11)$$

*For smaller number of n, we get similar formula, [5].

For common materials such as iron in the range of -100°C and 300°C, the value of (m+1)/(m+2) is from 0.85 to 0.71, rather independent of temperature. Thus with respect to temperature dependence of da/dN, equation (11) can be rewritten as:

$$\ln \frac{da}{dN} = \ln\left(\frac{A_2}{f^{\lambda}}\right) + b_o \ln\Delta K_1 - \frac{U_2 - a_o \ln\Delta K_1}{kT} \tag{12}$$

where A_2, a_o and b_o are material constants.

Comparison of the Theory with Experimental Data

1. The Power Exponent of Stress Intensity Factor δ

It is to be noted that as far as the power relation of da/dN and stress intensity factor are concerned, both equation (9) and equation (11) can be expressed as

$$da/dN = B_1 \Delta K_1^{\delta} , \tag{13}$$

which is the well known experimental result, [10]. For m = 1-4, we get $\delta \equiv (m+1)^2/(m+2) = 1.3 \sim 4.2$. These values are reasonable compared with the experimental data, [11].

2. The ΔK_1 and Temperature Dependence of da/dN

From recent experimental data for aluminum alloy, [12], with the stress intensity factor ΔK_1 as parameter, the logarithm of da/dN is plotted against 1/T (Arrhenius diagram) in Figure 8. It can be seen from the figure that in the range of higher values of ΔK_1 (or higher rate of da/dN) the intercept values of the straight line of da/dN with the coordinate axis at 1/T = 0 is approximately linear function as to $\ln \Delta K_1$, which is in good agreement with equation (12), that is,

$$\ln\left(\frac{A}{f^{\lambda}}\right) + b_o \ln\Delta K_1 .$$

On the other hand, for the range of lower level ΔK_1 (or lower rate of da/dN) the intercept value is one and the same value with stress intensity factor ΔK_1 which is in good accord with models based on microcrack nucleation at the crack tip [13], as expressed by an equation of the type

$$\ln \frac{da}{dN} = \ln\left(\frac{A_1}{f}\right) - \frac{U_1 - a_1 \ln\Delta K_1}{kT} , \tag{14}$$

where A_1 is a material constant.

3. Frequency Dependence

Experimental data show that da/dN is proportional to $f^{-\lambda}$ and λ experimentally obtained is 0.1 ~ 0.2 for steel [14] and 0.1~0.5 for aluminum alloys [14], [15], in air at room temperature. Hence the frequency dependence given by such type equation as equation (9) or equation (11) is also in reasonable accord with observations, as is the value of the power coefficient, (Figure 9).

4. The Relation Between the Proportional Constant B_1 and the Power Exponent δ

In equation (13) it can be seen from equation (9):

$$B_1 = B/(\sqrt{\varepsilon}\mu)^{\delta} . \tag{15}$$

From equation (15), we get

$$\log B_1' = \log B - \delta \cdot \log(\sqrt{\varepsilon}\mu) . \tag{16}$$

Such type as equation (16) is in good agreement with the experimental relation [16] between B_1 and δ as shown in Figure 10, as is the value of tangent of log B_1 versus δ, taking $\varepsilon = 1.5 \times 10^{-4}$ mm for steel.

5. Observations on Fatigue Crack Growth under Mode II Loading

The experiment [17] shows that in fatigue under Mode II loading the crack growth will occur in half the cycle during which the effective shear stress is exerted in such direction as the emission of dislocation can be realized from the crack tip, (Figures 11 ~ 13). These observations support the validity of the theory proposed.

Discussion

Let us consider the case for elastic-plastic crack. In this case

$$\sigma_{\ell} = f(\beta)\sigma_{cy}\left(\frac{\Delta K}{\sigma_{cy}\sqrt{\varepsilon}}\right)^{\frac{2\beta}{1+\beta}} \tag{17}$$

is used [18] in replace of $\Delta K_1/\sqrt{\varepsilon}$ as applied local stress in equation (9). σ_{cy}, β, and f(β) denote the initial yield stress in cyclic straining (not static yield stress), the cyclic strain hardening exponent and some function of β, respectively. Thus the crack growth rate becomes:

$$\frac{da}{dN} \propto \left(\frac{\Delta K_1}{\sqrt{2\varepsilon}\,\sigma_{cy}}\right)^{\frac{2\beta}{1+\beta}\,\frac{(m+1)^2}{m+2}} \tag{18}$$

For β = 0.08 ~ 0.3 and m = 4 ~ 10, the power exponent becomes 0.6 ~ 5, which may be still reasonable.

Also, the theory may be extended for the case in which COD has some finite value at the instant of tensile stroke, (Figure 14). Denoting this initial COD and dislocation density near the crack tip by L_1 and ρ_1, respectively, then the COD u corresponding to the crack growth rate is given by $u = L_1\sqrt{\rho_1}nb$. On the other hand, ρ_1 is experimentally expressed by $\rho_o + M\varepsilon_{sp}$, [19], where ε_{sp} and M are plastic strain and proportional constant, respectively. Assuming ρ_1 is similarly expressed by the cyclic plastic strain εp, expressing εp in terms of σ_{ℓ} based on cyclic stress-strain relation and using equation (17), then the crack growth rate becomes:

$$\frac{da}{dN} \propto \left[\frac{\Delta K_1}{\sqrt{2\varepsilon}\,\sigma_{cy}}\right]^{\frac{2\beta(m+1)^2}{1+\beta(m+2)} + \frac{1}{1+\beta}} \tag{19}$$

For $\beta = 0.08 \sim 0.3$ and $m = 4 \sim 10$, the power exponent becomes $2.0 \sim 5.0$, which may be still reasonable.

CONCLUSIONS

Combined micro and macro fracture mechanics approach has been made to the criterion for brittle fracture and fatigue crack growth as typical examples of so called time independent and dependent fracture respectively.

The criterion for crack propagation in brittle fracture obtained leads to apparently similar one to that by linear elasticity fracture mechanics in fairly good approximation. However, it is quite different in that it is expressed in terms of both micro and macro parameters and is applicable to nonlinear problems also.

Dynamic fatigue crack growth rate obtained leads to apparently similar one to usual experimental formula of power type. However, it quite differs from it, because of being expressed in terms of both micro and macro parameters, temperature and cyclic frequency.

The theories are in good accord with experimental data.

ACKNOWLEDGEMENTS

We would like to thank Dr. A. Kamei for general discussions.

REFERENCES

1. YOKOBORI, T., "Methodologies of Fracture in Matter and Solids", to be published.
2. YOKOBORI, T., KAMEI, A. and KONOSU, S., Engineering Fracture Mechanics, 8, No. 2, 1976, 397.
3. YOKOBORI, T. and KONOSU, S., Preprint Japan Soc. Mech. Engrs. (in Japanese), No. 760-2, 1976, 85.
4. YOKOBORI, T., YOKOBORI, A. T., Jr. and KAMEI, A., Phil. Mag., 30, 1974, 367.
5. YOKOBORI, A. T., Jr., YOKOBORI, T. and KAMEI, A., J. Appl. Phys., 46, 1975, 3720.
6. LAIRD, C., Am. Soc. Test. Mat., STP No. 415, 1967, 137.
7. NEUMAN, P., Act. Met., 17, 1969, 1219.
8. RICE, J. R. and THOMSON, R., Phil. Mag., 29, 1974, 73.
9. PREKEL, H. L. and CONRAD, H., Acta Met., 16, 1968, 337.
10. PARIS, P., An Interdisciplinary Approach Fatigue, J. J. Burk et al, Editors, 1964, 107.
11. MILLER, G. A., Trans. ASM, 61, 1968, 442.
12. YOKOBORI, T. and AIZAWA, T., Int. J. Fracture, 9, 1973, 489.
13. YOKOBORI, T., Physics of Strength and Plasticity, A. S. Argon, Editor, MIT Press, 1969, 327.
14. YOKOBORI, T. and SATO, S., Engn. Frac. Mech., 12, 1976, 158.
15. HARTMAN, A. and SCHIJVE, J., Ibid, 1, 1970, 615.
16. YOKOBORI, T., KAWADA, I. and HATA, H., Rep. Res. Inst. Strength and Fracture of Materials, Tohoku Univ., Sendai, Japan, 9, 1973, 35.
17a. YOKOBORI, A. T., Jr., YOKOBORI, T. and KAMEI, A., Trans. Japan Soc. Mech. Engrs., (in Japanese), (to be published).
17b. YOKOBORI, T., KAMEI, A. and YOKOBORI, A. T., Jr., Int. J. Frac., 12, 1976, 158.
18. RICE, J. R., J. Appl. Mech., 34, 1967, 287.
19. KEH, A. S. and WEISSMAN, S., "Electron Microscopy and Strength of Crystals, Interscience Pub., New York, 1963, 231.

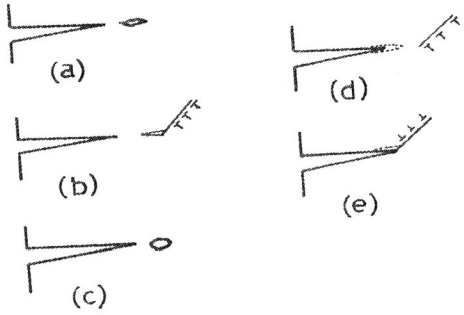

Figure 1 The Classification of the Mechanism of Crack Growth [1]

Figure 1 (b') As a Modified Model of Figure 1 (b), Figure 1 (b') can be considered. Especially for Brittle Fracture under Mode I at Plain Strain, Figure 1 (b') may be more realistic, and, thus, it is Needed to Analyse the Interaction for This Model

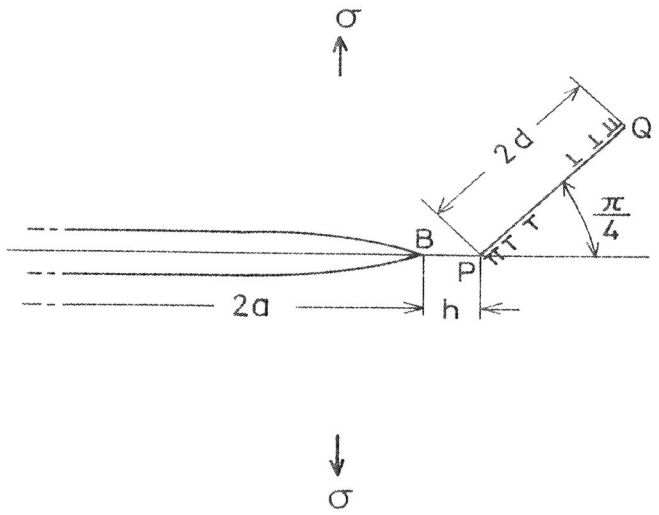

Figure 2 A Model of Crack Growth by Interaction of Crack and Slip Bands for Brittle Fracture

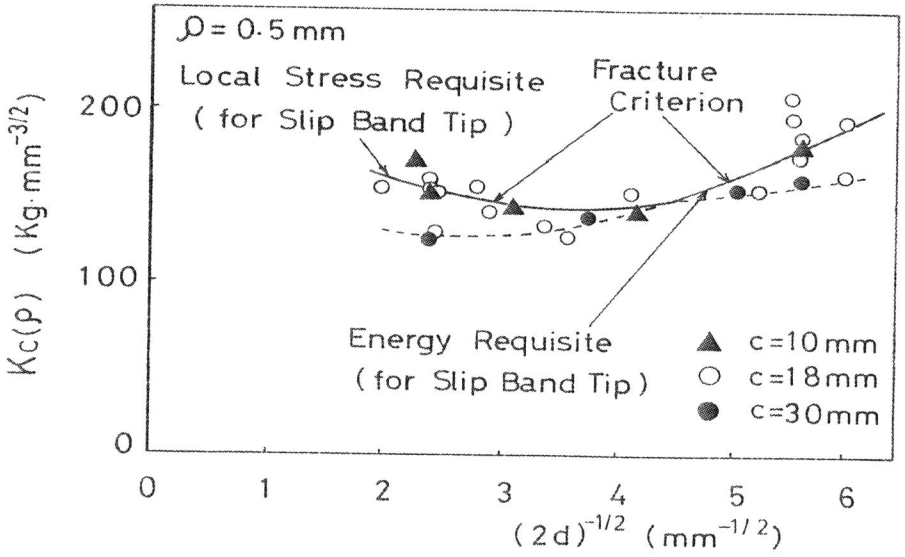

Figure 3 An Example of Grain Size Dependence of Brittle Fracture Stress or Fracture Toughness [3]

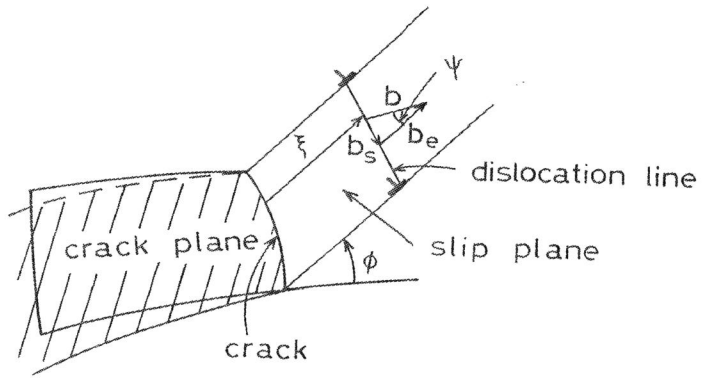

Figure 4 Schematic Illustration of the Relative Configuration of Dislocation and Crack

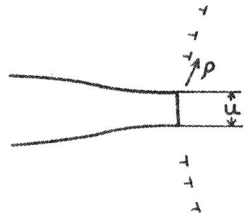

Figure 5 COD induced by Dislocation Emission from the Tip of Fatigue Crack

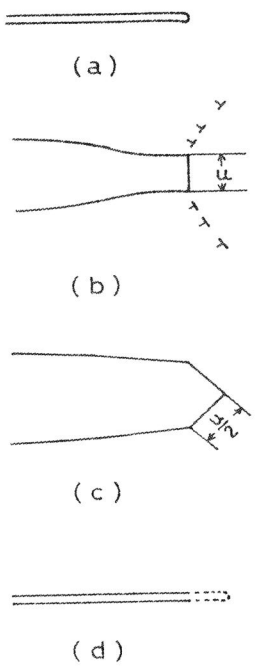

Figure 6 A Model of Fatigue Crack Growth in Terms of Dislocation Groups Dynamics Using Blunting and Resharpening Mechanism

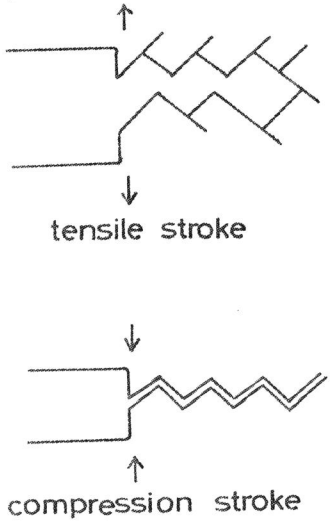

Figure 7 A Model of Fatigue Crack Growth in Terms of Dislocation Groups Dynamics Using Coarse Slip Mechanism

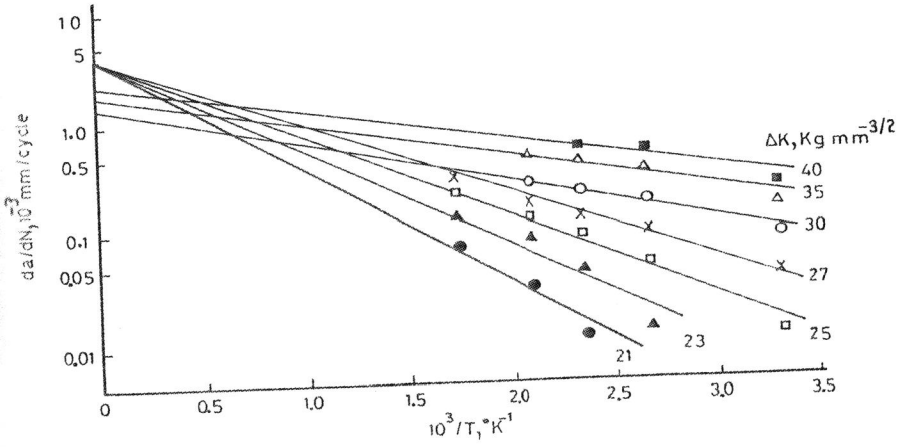

Figure 8 Comparison of the Theory with the Experimental Relation Between da/dN and 1/T for Aluminum Alloy at High Temperatures. The data was replotted from Reference [12]. The straight line for the Value of ΔK_I larger than 30 kg/mm$^{-3/2}$ corresponds to Equation (12), and for lower than 30 kg/mm$^{-3/2}$ corresponds to Equation (14) given by Nucleation Theory [13]

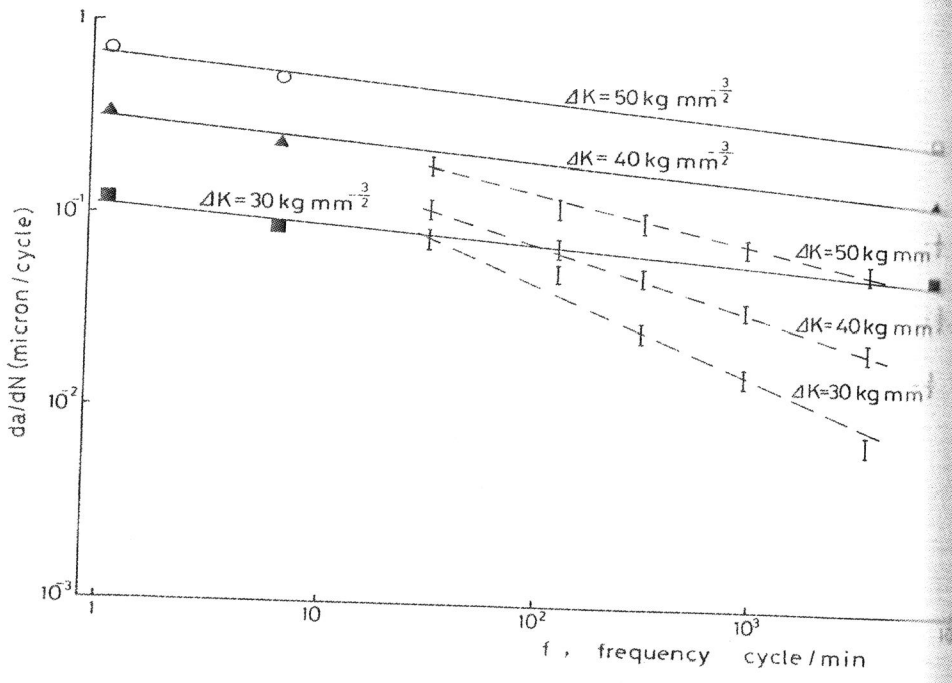

Figure 9 Fatigue Crack Growth Rate as a Function of Frequency in Aluminum Alloy in Air at Room Temperature. Solid Line: replotted from Reference [14]. Dotted Line: replotted from Reference [15].

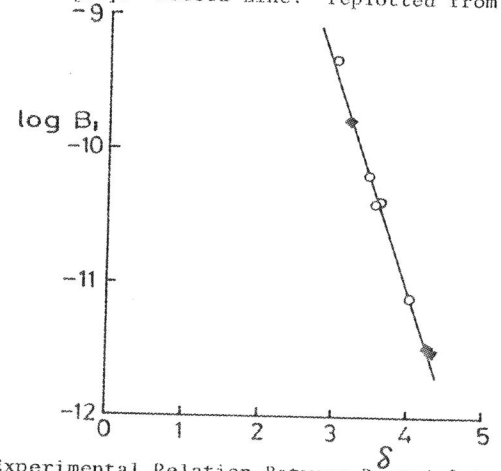

Figure 10 The Experimental Relation Between B_1 and δ in equation $da/dN = B_1(\Delta K)^{\delta}$, [16]. Each data have been obtained by changing Ferrite Grain Size. Hollow Circle: 0.05% C steel, Solid Circle: 0.08% C Steel

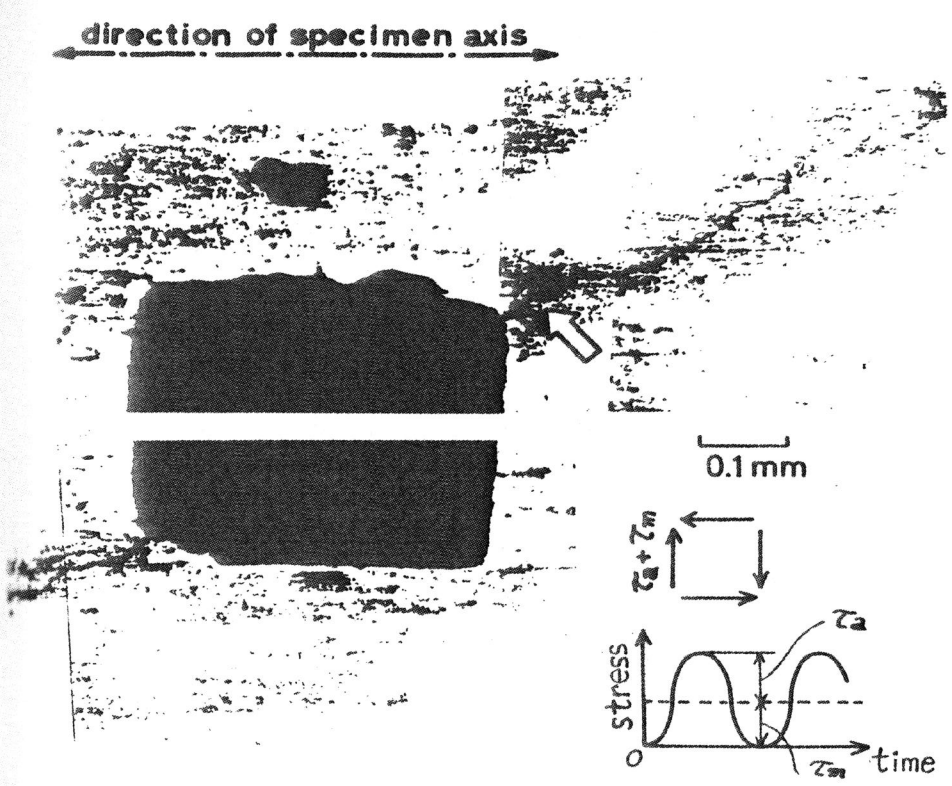

Figure 11 Fatigue Crack Growth in Thin-Walled Hollow Cylindrical Specimen (5083-PO aluminum alloy) under Reversed Torsion with Mean Stress τ_m equal to Stress Amplitude τ_a [17a]

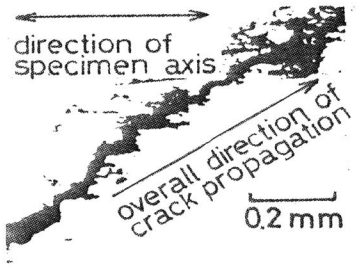

Figure 12 Magnification of the Crack Growth Pattern Pointed by the Arrow as Shown in Figure 11 [17a]

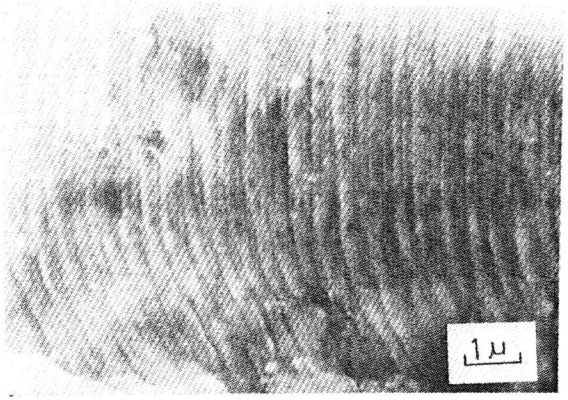

Figure 13 Striation-Like Pattern on the Fracture Surface [17a]

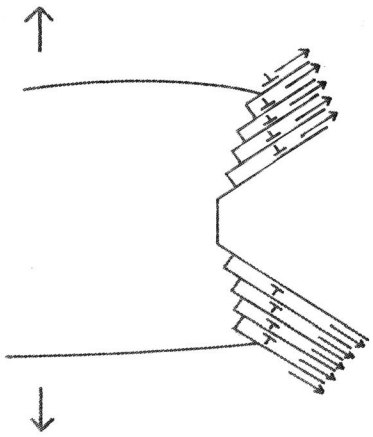

Figure 14 A Model of Fatigue Crack Growth in Terms of Dislocation Groups Dynamics in the Case of COD having Initial Finite Length at Start Point of each Tensile Stroke

Table 1 Classification of Crack Growth or Fracture

Micromechanism of crack growth or fracture	Separation of opposed atoms normal to the atomic planes by tensile stress		Slipping between opposed atoms parallel to the atomic planes by shear stress	
Class	Type 1	Type 2	Type 3	Type 4
Thermal activation	No or nearly No	Yes	No or nearly No	Yes
Time dependent	No or nearly No	Yes	No or nearly No	Yes
Fracture aspect	Brittle fracture and some of ductile fracture under one and unidirectional loading	Some of fatigue fracture and creep fracture. Stress corrosion cracking. Some of ductile fracture	Some of ductile fracture under one and unidirectional loading	Some of fatigue fracture, creep and ductile fracture
The Criterion for crack growth or fracture	Given by critical one of the two requisites: energy and local critical stress	Given by one requisite including both energy and local critical stress condition	Given by critical one of the two requisites: energy and local critical stress	Given by one requisite including both energy and local critical stress condition

Table 2 Criterion Derived for the Brittle Fracture

(a) For the Case of the Main Crack Tip Radius Being Large

	$K_{IC} = \sqrt{2E\gamma_p^*}$	
	For Smaller Grain Size Range Energy Requisite	For Larger Grain Size Range Critical Local Stress Requisite
Low Slip Band Density	$\gamma_p^* \simeq \frac{\rho+4h}{E\left\{1+0.2n^*\sqrt{\frac{4d}{\rho+4h}}\right\}^2}\left[\tau_i+\sqrt{\frac{4E(\gamma_s+\gamma_e)}{\pi\kappa(2d)}+\tau_i^2}\right]^2$	$\gamma_p^* \simeq \frac{\rho+4h}{E}\left[4\sqrt{\frac{E}{2d}}\frac{\sigma_{th}}{n^*}+2\tau_i\right]^2$
High Slip Band Density	$\gamma_p^* \simeq \frac{\{\rho+1.5(h+d)\}\sigma_Y^2}{E}\left[\frac{\tau_i+\sqrt{\frac{4E(\gamma_s+\gamma_e)}{\pi\kappa(2d)}+\tau_i^2}}{\sigma_Y}\right]^{\frac{1+\lambda}{\lambda}}$	$\gamma_p^* \simeq \frac{\{\rho+1.5(h+d)\}\sigma_Y^2}{E}\left[\frac{4\sqrt{\frac{E}{2d}}\frac{\sigma_{th}}{n^*}+2\tau_i}{\sigma_Y}\right]^{\frac{1+\lambda}{\lambda}}$

ρ, σ_Y, n^*, λ, γ_s, γ_e, τ_i and σ_{th} have the same meaning as in Reference [2].

(b) For the Case of the Main Crack Tip Being Very Small

	$K_{IC} = \sqrt{2E\gamma_p^*}$	
	For Smaller Grain Size Range Energy Requisite	For Larger Grain Size Range Critical Local Stress Requisite
Low Slip Band Density	$\gamma_p^* \simeq \frac{50n^{*2}d}{E(n^*\sqrt{d}+10\sqrt{\rho+4h})^2}\left[\frac{\sqrt{\pi a}}{100}\tau_i+\sqrt{\frac{4E(\gamma_s+\gamma_e)(\rho+4h)}{\kappa n^{*2}(2d)}}\right]^2$	$\gamma_p^* \simeq \frac{50n^{*2}\rho hd}{E\left\{n^*\sqrt{\rho d}+2\sqrt{h}(1+15\sqrt{\rho+4h})\right\}^2}$ $\times\left[2\sqrt{\frac{\rho+4h}{2d}}\frac{\sigma_{th}}{n^*}+\left\{\sqrt{\frac{\rho+4h}{h}}(1+0.004n^*\sqrt{\frac{a}{\rho+4h}})+0.03\sqrt{\frac{a}{\rho}}\right\}\tau_i\right]^2$
High Slip Band Density		$\gamma_p^* \simeq \frac{\{\rho+1.5(h+d)\}\sigma_Y^2}{E\left\{1+\frac{4}{n^*}\sqrt{\frac{h}{2d}}\left(1+\frac{1.5}{\rho}(h+d)\right)^{\frac{1}{1+\lambda}}\right\}^{\frac{1+\lambda}{\lambda}}}$ $\times\left[\frac{4\sqrt{\frac{h}{2d}}\frac{\sigma_{th}}{n^*}+2\tau_i}{\sigma_Y}\right]^{\frac{1+\lambda}{\lambda}}$

$\kappa = 1 - \nu^2$: plane strain